Mon. Not. R. Astron. Soc. 000, 000–000 (0000) Printed 7 August 1997

A Multiwavelength Study of the Starburst Galaxy NGC 7771

Richard I. Davies[1], Almudena Alonso-Herrero[1,2], and Martin J. Ward[1,3]
[1] *Astrophysics, Nuclear Physics Building, Keble Road, Oxford, OX1 3RH, UK*
[2] *Steward Observatory, University of Arizona, Tucson, AZ 85721, USA*
[3] *Department of Astronomy and Physics, University of Leicester, Leicester, LE1 7RH, UK*

Accepted 1999 December 31. Received 1999 January; in original form 7 August 1997

ABSTRACT

We present a multiwavelength study of the interacting starburst galaxy NGC 7771, including new optical and ultra-violet spectra and a previously unpublished soft X-ray *ROSAT* image and spectrum. The far-infrared, radio, and X-ray fluxes suggest that a massive burst of star-formation is currently in progress but the small equivalent width of the Balmer emission lines (equivalent width H$\alpha \approx 100$ Å), the weak UV flux, the low abundance of ionised oxygen, and the shape of the optical spectrum lead us to conclude that there are few O stars. This might normally suggest that star-formation has ceased but the galaxy's barred gravitational potential and large gas reserves imply that this should not be so, and we therefore consider other explanations. We argue that the observations cannot be due to effects of geometry, density bounded nebulae, or dust within the nebulae, and conclude that a truncated IMF is required. The dwarf galaxy NGC 7770 appears to be in the initial stages of a merger with NGC 7771, and the resulting tidal perturbations may have induced the apparent two-armed spiral pattern, and driven a substantial fraction of the disk gas inwards. The presence of a bulge in NGC 7771 may be moderating the starburst so that, while still occuring on a large scale with a supernova rate of 0.8–1 yr^{-1}, it is less violent and the IMF has a relatively low upper mass limit. We find that there is a cluster of stars obscuring part of the starburst region, and we offer an explanation of its origin.

Key words: Galaxies: starburst – Galaxies: individual: NGC 7771

1 INTRODUCTION

The term 'starburst' was originally coined by Weedman et al. (1981) to indicate qualitatively that a galaxy is undergoing a period of intense star formation. It still lacks a precise definition and provides a blanket covering for all regions that have an above normal star formation rate. In particular for interacting galaxies, it includes star formation enhanced by any process ranging from a mild perturbation to a collision. When the data available on a certain system is limited and the initial mass function (IMF) must be guessed at, often the assumption is that the starburst has a Salpeter IMF with masses in the range 0.1–100$M_\odot$. While this may be a reasonable starting point for analysis of starbursts, it has not been established that it can be applied directly to all star-forming regions. Indeed there is evidence to the contrary.

There has been some effort to constrain the IMF mass limit and Charlot et al. (1993) have investigated the evolution of starbursts with high lower mass cutoffs. Scalo (1989) reviewed the evidence for top-heavy IMFs resulting in a deficiency of low-mass stars in starbursts. He concluded that most starburst galaxies do not require a top-heavy IMF, if the upper mass limit (M_u) is large enough ($M_u > 80$–$100M_\odot$). In a significant fraction of galaxies this was not the case and so to avoid excessive masses of newly formed stars the lower mass limit (M_l) must be higher, perhaps as much as $M_l = 3$–$10M_\odot$ as was found by Rieke et al. (1980) for the starburst in M82. Which of these situations applies in any particular case has bearing on the masses involved and the efficiency with which stars are formed, as well as the question of whether perturbations and heating associated with enhanced star formation rates inhibits the formation of low-mass stars. More recently Doyon et al. (1992) suggested that the ratio HeI 2.058μm/Brγ might be a reliable indicator of M_u for ratios less than $\sim$0.5, corresponding to $M_u \leq 40M_\odot$, although Shields (1993) pointed out that the neutral helium to hydrogen fraction decreases with increasing effective temperature.

Evidence for truncated IMFs in starburst galaxies is very limited at present, due partly to the number of factors

which must be considered, and also because many starbursts may indeed have IMFs that are not significantly truncated. Perhaps the best documented case of a truncated IMF is in M82, for which the upper mass cut-off has been found to be about $30M_{\odot}$ (Rieke et al. 1980, Puxley et al. 1989, and Doyon et al. 1992); more recent work on this galaxy by Rieke et al. (1993) using updated models has shown that while low mass star formation appears to be suppressed, the abundance of higher mass stars is consistent with that found in the solar neighbourhood. The debate on this galaxy continues and, by measuring mid-infrared line ratios, Achtermann & Lacy (1995) place an upper limit on the effective temperature of the hottest stars as ~35,000 K, equivalent to stars of ~20 $M_{\odot}$. The argument for unusual IMFs been further supported by Gehrz et al. (1983), Wright et al. (1988), and Doyon et al. (1992) who have found other galaxies where the mass function is severely truncated at both ends.

In this paper we consider the case of NGC 7771, an SB(s)a galaxy interacting with NGC 7770, at a redshift of 4345 km s^{-1} (Soifer et al. 1987) corresponding to a distance of 87 Mpc (H_0 = 50 km s^{-1} Mpc^{-1}). This galaxy has an infrared luminosity of $\log L/L_{\odot} = 11.6$ ranking it amongst some of the most luminous infrared galaxies known. The stellar origin for this power output and the galaxy's relative closeness with respect to other comparably luminous objects, makes it an ideal candidate for the study of star-formation on a massive scale. Our observations reveal that the central region of NGC 7771 has unusual characteristics which could be explained in a variety of ways, one of which requires a truncated IMF.

This paper is organised as follows: In Section 2 we present and discuss the optical spectrum, in Section 3 the UV spectrum, and in Section 4 the X-ray emission. These are put into context with each other and discussed with reference to detailed starburst models in Section 5. Finally, in Section 6 we present our conclusions.

2 OPTICAL SPECTRUM

2.1 Observations

The optical spectrum was obtained using the Intermediate Dispersion Spectrograph (IDS) on the 2.5-m Isaac Newton Telescope (INT) on November 12, 1993 with a 900s integration. The configuration was a 1.5 arcsec wide long-slit centered on the optical peak and oriented at position angle 59°, shown schematically in Figure 1. The spatial resolution along the slit was 0.6 arcsec/pixel although the PSF of the standard star showed that the seeing was about 1.5 arcsec. The spectral resolution of $R \sim 1000$ was matched to the 3.05 Å/pixel, yielding an effective resolution of about 6 Å (FWHM) and covering the range approximately 3600–6900 Å.

Data reduction was performed with IRAF, following standard procedures. After bias subtraction and flatfielding, the pixels affected by cosmic rays were rejected and interpolated over. The background was fitted using regions away from the bright galaxy, and subtracted. Wavelength calibration was carried out using a Cu-Ar arc lamp and then spectra were extracted, corrected for atmospheric extinction, and flux calibrated by a standard star observed at a similar airmass.

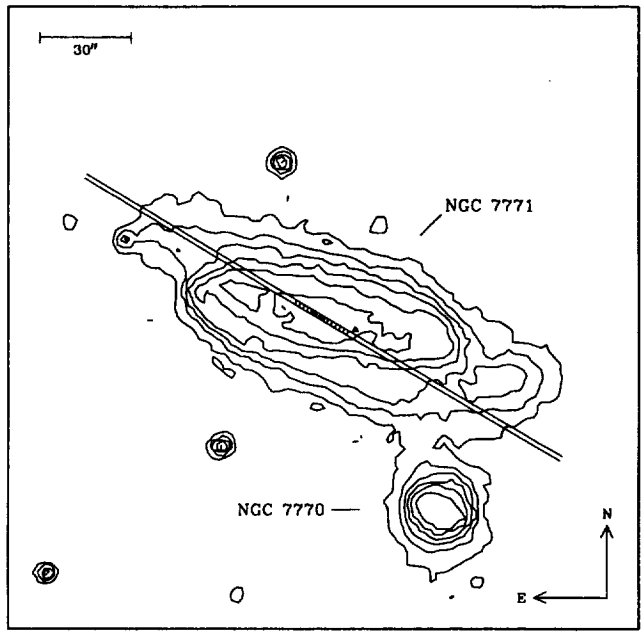

Figure 1. Contour plot of NGC 7771 and NGC 7770 in the optical from the Digitised Sky Survey showing the orientation of the 1.5 arcsec wide long-slit. The shaded region of the slit shows the section that has been mapped in Figure 2; the two bars parallel to the slit indicate the two regions discussed in Section 2.3.

2.2 Spatial Mapping

In order to make the most use of the spatial information that a long-slit affords, the central 19.5 arcsec was divided into a series of 1.5 arcsec (630 pc) apertures. For each of the resulting spectra measurements were made of the total integrated flux of the spectrum, the slope of the continuum, the Hα line flux and equivalent width ($EW_{H\alpha}$), and where possible the Hβ line flux.

Figure 2 shows in (a) the total brightness, computed as simply the total flux detected in each aperture normalised to 10 for the central one, and in (d) the continuum colour, i.e. the ratio of the continuum flux density at Hα to that at Hβ with the dotted line representing a flat continuum. Both quantities show clearly that along the slit, the region within ±4 arcsec of the peak, about 3 kpc across, is brighter and bluer, indicative of a starburst nucleus. The red outer regions are consistent with an old evolved stellar population similar to that found in galactic bulges. The Hα flux and equivalent width, in (b) and (e) respectively, show immediately that this is not the complete picture. In both diagrams the optical brightness has been over-plotted with a dashed line and arbitrary scale for comparison. To explain why these do not peak at the same place, we first consider the northeast side (negative offset). The Hα flux increases dramatically at the same point as the optical brightness, which is also where the continuum becomes much bluer. This suggests that the nucleus hosts a cluster of hot young OB stars which are producing a large ionising flux. In such a situation we might expect $EW_{H\alpha}$ to change more slowly, which is the case, as further from the nucleus the continuum becomes more dominated by older redder stars. However, to the southwest (positive offset) the Hα flux decreases abruptly. That the $EW_{H\alpha}$ also suffers a marked cut-off suggests that the stellar

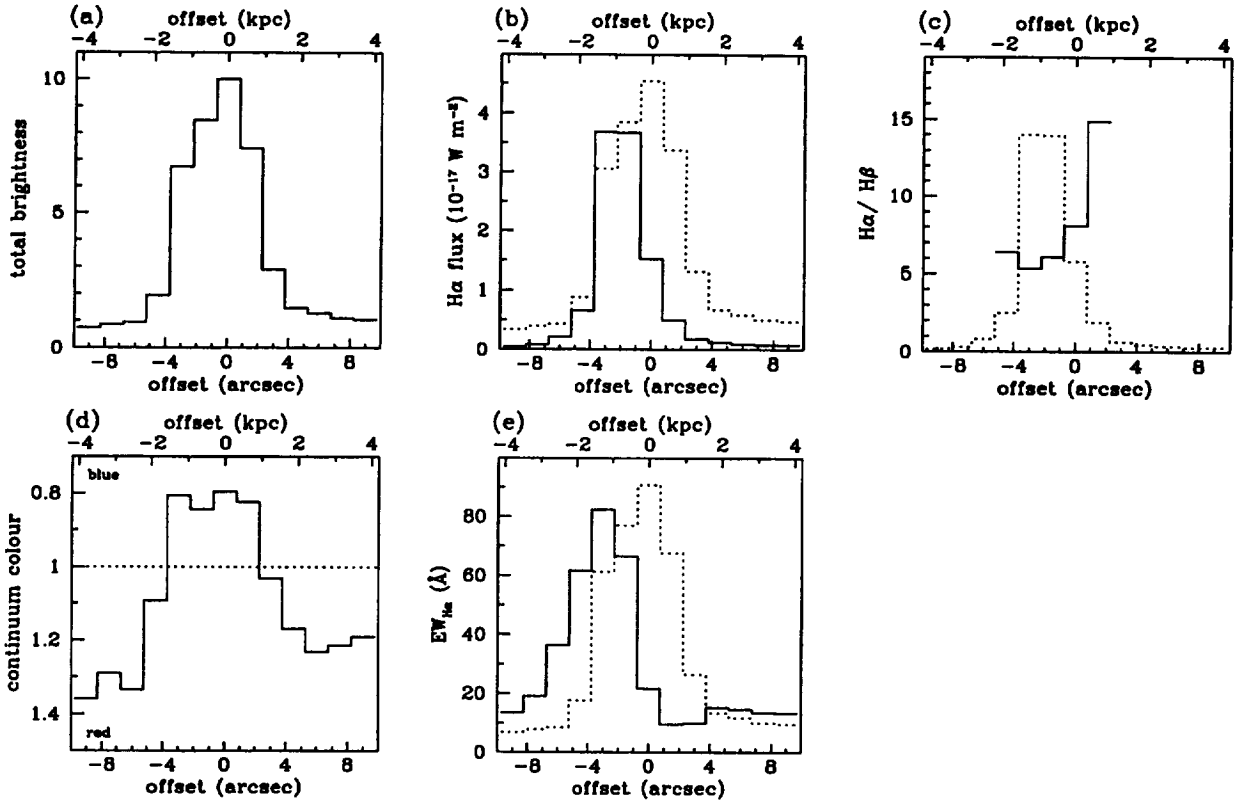

Figure 2. Mapped region of the long-slit showing the variation along the slit. Negative offsets are to the northeast and positive offsets southwest. The individual frames (described in the text in more detail) are: (a) total optical brightness, (b) observed Hα flux, (c) ratio Hα/Hβ, (d) continuum colour, and (e) Hα equivalent width.

population changes suddenly from hot OB stars to cooler non-ionising ones, but this cannot be correct because the continuum colour shows that the stars are still very blue. To understand it further we need to know how the extinction varies across the nucleus. Since this can be calculated from the Balmer decrement, we have shown the ratio Hα/Hβ in (c), although it could only be measured for the 5 apertures in which Hβ was strong enough to detect. The Hα flux has been over-plotted (dotted line and arbitrary scale) to show that it is strongest where the extinction is lowest ($A_V \approx 2$ mag), and that the cut-off occurs where the extinction increases rapidly by 2–3 magnitudes. The data plotted are maximum ratios as there is considerable Hβ absorption, especially to the southwest, which could not always be accurately deblended from the emission line flux. It is notable that the dereddened Hα flux is approximately constant over the region where it can be calculated, suggesting that the starburst does indeed cover the entire region indicated by the bluest continuum colours. There might then be either a dust lane or a cluster of non-ionising stars obscuring part of this, and causing the extra extinction. The effect of a dust lane would be to redden the continuum and reduce the detected flux. Since neither of these happen, and since also there is no evidence for a dust lane on the optical image, we conclude that the obscuration is due to a cluster of stars. In order to investigate these two regions with a higher signal-to-noise ratio, we extracted two further non-overlapping spectra, both 2.4 arcsec wide. The first, denoted region 1, was offset to the northeast by 3 arcsec, to look at the starburst where it was least obscured; the second, denoted region 2, was centered on the optical peak, corresponding to the obscuring cluster and high extinction to the starburst. These two regions are indicated in Figure 1 by the two thick lines drawn parallel to, and within, the slit.

Although the obscuration clearly varies considerably across the mapped section of the nucleus, the average extinction is a useful quantity which we estimate to be $A_V = 2.3$ mag, noting that it will be biassed towards lower values that are more easily measured. We have shown that the starburst, although partly obscured, extends with approximately constant surface brightness across the whole 7.5 arcsec nucleus at the orientation of the slit. In this limited region, we calculate an extinction corrected surface brightness for the Hα emission of 4.0×10^{-16} W m^{-2} kpc^{-2}.

2.3 Two Nuclear Regions

The spectra for both regions, smoothed with a Gaussian filter of FWHM ~6 Å are presented in Figure 3 on the same scale to allow direct comparison. The most obvious differences are that Region 1 is less reddened and Region 2 has greater Balmer absorption as well as a bluer continuum.

From the Balmer emission line decrement we find that in Region 1 $A_V = 1.9$ mag, while in Region 2 $A_V = 3.0$ mag. The extra obscuration is caused by the star cluster that is also responsible for the much enhanced Balmer absorption. The spectrum of this cluster is discussed in more detail later (see Section 2.4). The strengths of the detectable emission

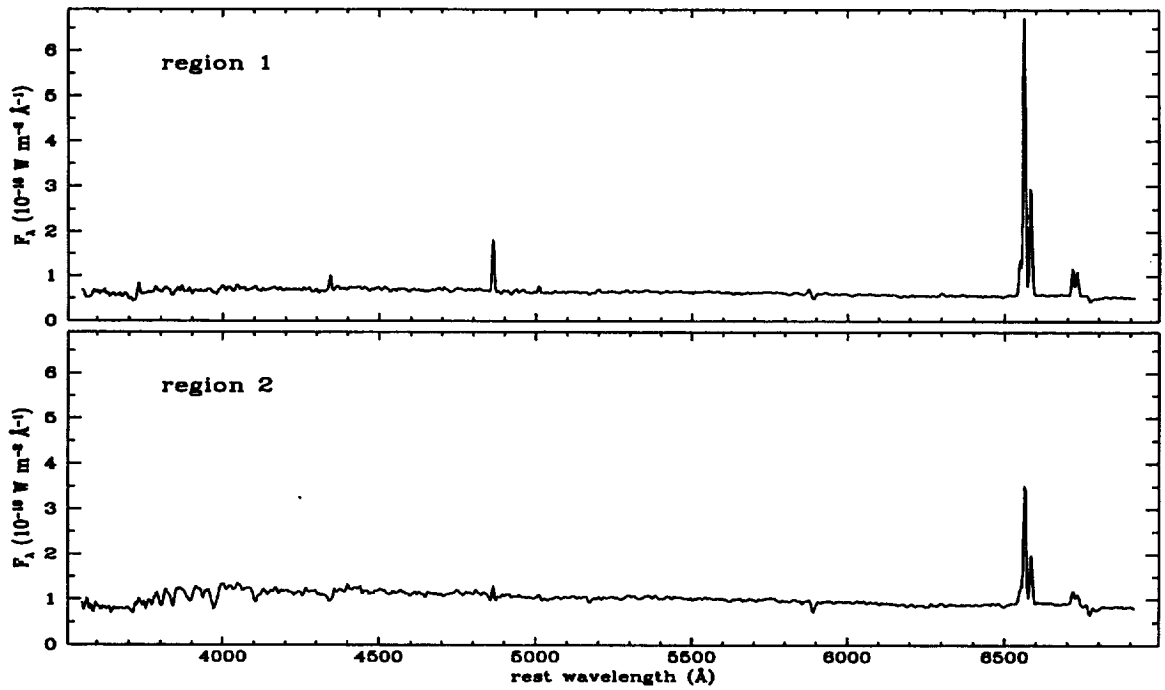

Figure 3. Spectra of the starburst where it is least obscured, Region 1, and where the obscuring cluster is covering it, Region 2. They are plotted on the same scale to emphasise the differences in both lines and continuum.

Table 1. Emission Lines

emission line		Region 1 F^1_{obs}	Region 1 $F^{1,2}_{corr}$	Region 1 EW (Å)	Region 2 F^1_{obs}	Region 2 $F^{1,3}_{corr}$	Region 2 EW (Å)
[SII]	λ6731	5.1	20	8.7	2.3	20	2.6
[SII]	λ6716	5.6	23	9.8	3.3	29	3.7
[NII]	λ6583	23.8	99	42.0	11.9	108	13.2
Hα	λ6563	60.3	253	106.5	28.6	262	[4]31.8
[NII]	λ6548	8.1	34	14.4	5.1	47	5.6
[OI]	λ6300	0.8	4	1.4	0.8	8	0.9
[HeI]	λ5876	1.0	5	1.6	0.2	3	0.2
[OIII]	λ5007	1.0	7	1.5	0.7	15	0.7
Hβ	λ4861	10.8	87	16.2	3.6	89	3.2
Hγ	λ4340	2.7	30	4.0	—	—	—
[OII]	λ3727	3.0	52	5.9	—	—	—

[1] observed and reddening corrected fluxes $\times 10^{-18}$Wm^{-2} in a 2.4 arcsec × 1.5 arcsec aperture. 1σ errors, not including deblending, are typically ±0.3 in the same units.
[2] 1σ errors typically ±2 at Hβ and ±1 at Hα.
[3] 1σ errors typically ±6 at Hβ and ±2.5 at Hα.
[4] Veilleux et al. (1995) find that $EW_{H\alpha}$ = 26Å in a 2 arcsec × 2 arcsec aperture centred on the optical peak.

lines before and after appropriate dereddening, as well as their equivalent widths, are presented in Table 1.

Kim et al. (1995) find Hα/Hβ = 21.4 in a 2 arcsec × 2 arcsec aperture centred on the nucleus, considerably larger than our value of 8.1 for Region 2, due in part to our measuring a larger equivalent width, 4.6 Å, for the Hβ absorption. We do, however, measure a similar NaI absorption of 3.3 Å in the same region.

A simple test can be performed to determine whether the emitting gas is photoionised by OB stars or a power-law continuum source. We employ the diagnostic diagrams described in Fruscione & Griffiths (1991), which compare the dereddened ratios shown in Table 2. Plotting the line ratios on the diagrams shows clearly that both regions are starbursts. Since the Hα surface brightness is the same and they are in close proximity with no obvious break between them, it seems reasonable to conclude that they are in-fact part of the same starburst. The difference in reddening (ΔA_V = 1.1 mag) is entirely attributable to the obscuring cluster. Storchi-Bergmann et al. (1995) found for a sample of

Table 2. Emission line ratios

ratio	Region 1	Region 2
log [OIII]λ5007/Hβ	-1.08	-0.77
log [NII]λ6583/Hα	-0.41	-0.38
log [SII](λ6716 + λ6731)/Hα	-0.77	-0.73
log [OI]λ6300/Hα	-1.85	-1.50

Note: line ratios are corrected for reddening.

starbursts that log [OIII](λ4959 + λ5007)/H$\beta = -0.10^{+0.27}_{-0.90}$ (not corrected for extinction). Our values (which are the same within their 1σ errors) lie at the bottom end of this range, and are consistent with an effective temperature for the radiation field of the starburst of 35–40 $\times 10^3$ K, assuming solar metallicity (Evans & Dopita 1985).

An upper limit to the velocity dispersion implied by the widths of the lines can be estimated by comparing their FWHM to the instrumental FWHM of 287 ± 8 km s^{-1} (measured from the arc lines). We find that for Region 1 the FWHM of the six strongest lines is 291 ± 9 km s^{-1}, showing that they are unresolved; and for Region 2 the FWHM for the same lines is 370 ± 12 km s^{-1}. The limit on the velocity dispersion is therefore $\lesssim$200 km s^{-1}, in line with what we would expect for a nuclear starburst; we suggest a reason for the differing line widths in Section 5.4. The lack of any broad component suggests there is no outflow such as from supernovae induced winds (see Section 5.2). The heliocentric velocity of the lines is 4790 ± 80 km s^{-1}.

The ratio of the sulphur lines in the doublet can be used as a density diagnostic. We find that [SII]$\frac{\lambda 6716}{\lambda 6731}$ =1.1–1.4, typical of densities 100–500 cm^{-3}, consistent with those values found in other extragalactic HII regions (French 1980).

2.4 The Obscuring Cluster

Since the emission lines in the two regions are produced by the same starburst, we can redden the spectrum from Region 1 using $\Delta A_V = 1.1$ mag so that the emission lines correspond to those in Region 2 and then subtract it without further scaling. The residual will be the spectrum of the stars and dust that is obscuring the starburst in Region 2, and is shown in Figure 4 smoothed with a Gaussian of FWHM 9 Å.

The deep Balmer absorption is clearly shown. There also appears to be some residual Hα due to the difference in line-widths between the two regions; the overall excess emission in the line is very small. The continuum is very blue: the ratio of the continuum at Hα to that at Hβ is 0.68, more extreme than any in Figure 2(d). There can be very little foreground extinction since this would make the intrinsic spectrum even bluer, which would lead us to expect some of the stars contributing to it would be hot enough to create an HII region. In such a situation the Hα flux and equivalent width would not drop as abruptly as is seen.

We have used the stellar library of Silva & Cornell (1992) to synthesise this spectrum. By considering particular features of the spectrum it is possible to constrain the range of populations in the model. For example, the Balmer decrement (3700–4000 Å) is typical of A and B stars, whereas the absorption bands of MgI (5150–5200 Å) and NaI (5880–5900 Å) are indicative of K and M stars; and the CaI (4230 Å) and CaII (3900–4000 Å) absorption is most apparent in F stars. Lastly, the overall slope of the continuum must be matched and puts further limitations on the possible stellar classes present. Although this does not provide an entirely unique model, it does show broadly the fractional contributions from the various stellar types. The spectra in the stellar library are normalised at 5450 Å and it is at this wavelength that we find significant contributions from B, A, F, and G stars, but also enough optically faint K and M stars that these will dominate the mass. A small amount of reddening ($A_V = 0.3$ mag) is also required. The Hβ, Hγ, and Hδ absorption features indicate that the redshift of the object is 4800 ± 240 km s^{-1}, the same as the redshift of the emission lines in Section 2.3.

3 UV SPECTRUM

A UV spectrum was obtained with the International Ultraviolet Explorer (IUE) satellite on November 29 and 30 1994 with the long-wavelength (LWP) and short-wavelength (SWP) cameras respectively, in the large (10 arcsec × 20 arcsec) aperture. The resulting spectrum, extending from 3200 Å to 1200 Å, was extremely faint and so we were unable to distinguish or measure any line fluxes. In order to increase the signal-to-noise ratio we binned the data in 200 Å sections, 3 each for the LWP and SWP cameras. Because of this we have not shown the spectrum here explicitly although it is included in Figure 8 (see Section 5.1).

Kinney et al. (1993) looked at a sample of starbursts for which $\beta = -1.25 \pm 0.45$ ($F_\lambda = f_o \lambda^\beta$). NGC 7771 has $\beta = 0.56 \pm 0.18$ (weighted towards the fluxes with higher SNR), considerably redder than even the reddest in the sample of Kinney et al. (NGC 7552 with $\beta = 0.26 \pm 0.14$). One of the criterion for objects to be included in the sample was based on signal-to-noise ratio and hence the sample is mostly of galaxies with low reddening and strong UV flux. The UV spectra of objects in the sample are consistent with those of O and B stars. Naively then, NGC 7771 would appear to be a heavily reddened source. However, Kinney et al. discuss the effects of reddening on the UV spectrum. They claim that the optical depth is unlikely to be near unity. Rather the dust will be patchy, and optically thick enough that either the UV radiation has a completely free path or encounters dust and is totally absorbed. Thus the effect of dust is not to alter the shape of the spectrum, but simply to reduce the observed flux. This is supported by their inability to reproduce a typical blue spectrum by dereddening one of the red spectra, even with a variety of extinction laws. We conclude that the shape of the spectrum in NGC 7771 is not due to reddened flux from O and B stars, but is from A or B stars which it more closely resembles.

4 X-RAY DATA

Fabbiano (1989) suggests that the typical soft X-ray luminosity of starburst nuclei is on the order of 10^{32} W. NGC 7771 is unusual in having an X-ray luminosity of more than 10^{34} W (see below), and so we have included a section on the observations and possible origins of the emission.

NGC 7771 has been observed in soft X-rays with both the *Einstein* Observatory and *ROSAT*, but no hard X-ray

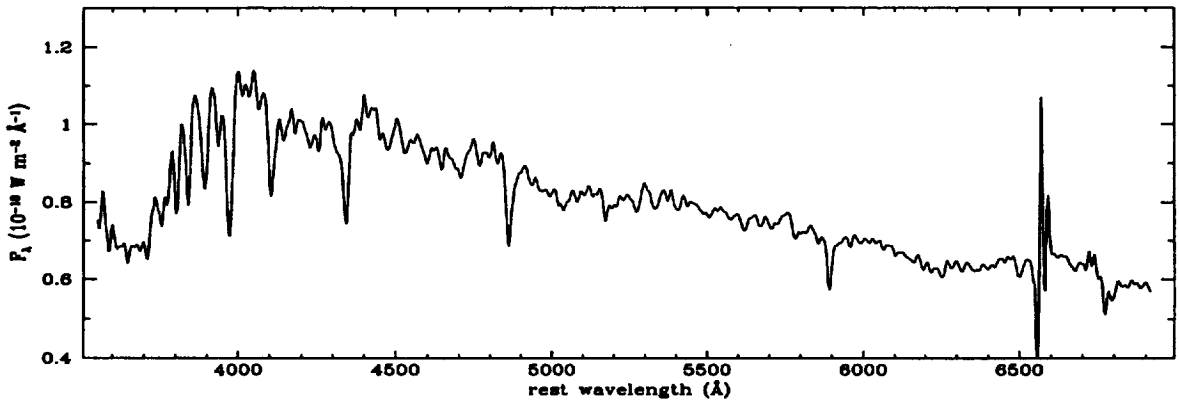

Figure 4. Spectra of the obscuring cluster, obtained by subtracting the suitably reddened spectrum of Region 1 from that of Region 2.

emission was detected by the HEAO-1 mission; for example the data presented in Rephaeli et al. (1995) have less than 1σ significance. All X-ray data includes contributions from NGC 7770 as well as NGC 7771 and we have not attempted to distinguish between them.

We have recalibrated the soft X-ray flux detected by the *Einstein* IPC device (0.16–3.5 keV) from the CDROM images. In a region with radius 210 arcsec we measure 100.2 ± 10 counts, agreeing well with the 104.7 measured by Fabbiano et al. (1992) for the same aperture. The hardness ratio, that is the relative contributions of 'hard' (0.81–3.5 keV) and 'soft' (0.16–0.81 keV) counts, for the galaxy is 0.36 ± 0.13. Together with the Galactic absorbing column of hydrogen, $N_{\rm H} = 3.96 \times 10^{20}$ cm^{-2}, it can be used to estimate the flux using an appropriate model. We choose the Raymond-Smith thermal plasma model with cosmic abundances and a temperature $kT = 1.7$ keV (from the hardness ratio) to give a luminosity of $5.4 \pm 0.5 \times 10^{34}$ W.

The galaxy was also observed by *ROSAT* on two occasions with the PSPC device: on December 16 1992 with a live-time of 7655 s, the count rate was 0.0151 ± 0.0020 s^{-1} in an aperture of radius 210 arcsec; and on July 10–13 1992 with a live-time of 4150 s, the count rate was 0.0181 ± 0.0043 s^{-1} for the same aperture.

The *ROSAT* PSPC X-ray images from both observations were aligned (with reference to several prominent objects in the field, and requiring sub-pixel shifts) and averaged, weighting each frame with its exposure time. The resulting image is shown in Figure 5 as contours (linear scale) superimposed on a grey-scale optical image. The 30-arcsec resolution of this image is better than that of the *Einstein* IPC (75 arcsec) and appears to show that, although the strongest emission is from the galactic centre, it extends throughout the galaxy's disk and possibly beyond. The emission to the south of the galaxy and the ridge which appears to join NGC 7770 may be effects caused by the PSF of the PSPC which is quite large with respect to the angular size of the galaxy (it is represented by the size of the scale bar). Emission from near the edge of the disk may appear to originate from outside it. Higher resolution imaging, such as with the HRI instrument, is needed to resolve this point.

The PSPC instrument has 256 channels which provide a certain amount of spectral coverage (0.1–2.4 keV). For the latter observation above we extracted this spectrum us-

Figure 5. Contours showing the X-ray emission detected by the *ROSAT* PSPC, centered on a grey-scale optical image taken from the Digitised Sky Survey. The PSPC has a FWHM resolution of 30 arcsec, as shown by the scale bar.

ing ASTERIX and corrected both source and background counts for vignetting and dead time. The background was subtracted using XSPEC, and channels 20–200 of the resulting spectrum were modelled. Due to the small total counts (only about 100 photons were detected) the spectral analysis is restricted and we do not quote formal errors. Instead the 'best-fit' models should be taken as in indication of the possible fits rather than as unique solutions. Two models, statistically indestinguishable by minimum χ^2 (reduced $\chi^2 = 0.4$), are shown in Figures 6 and 7 together with the data which has been binned to a level of 2σ or a maximum of 16 channels per bin. Figure 6 shows a power-law fit for which the best fitting parameters are an absorption column density $N_{\rm H} = 1.8 \times 10^{21}$ cm^{-2}, and a photon index $\Gamma = 3.5$. Figure 7 shows in (a) a fit with an absorption column density $N_{\rm H} = 4.5 \times 10^{20}$ cm^{-2} (similar to the galactic absorbing

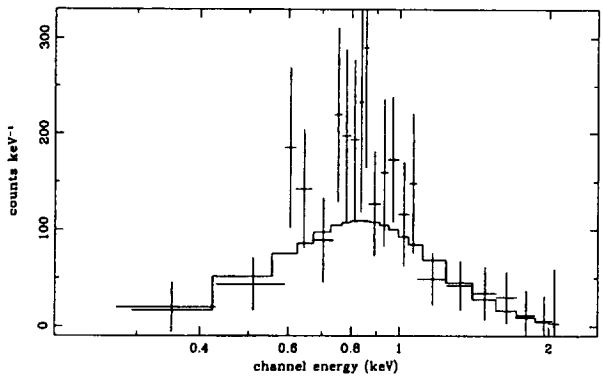

Figure 6. *ROSAT* PSPC X-ray spectrum (binned to a level of 2σ or a maximum of 16 channels) shown with the best-fit power-law model with absorption.

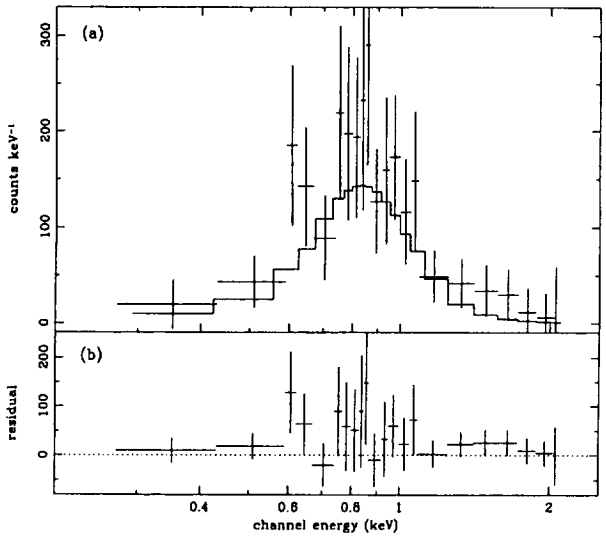

Figure 7. *ROSAT* PSPC X-ray spectrum (binned to a level of 2σ or a maximum of 16 channels) shown with best-fit Raymond-Smith hot plasma model with absorption. (a) shows the model, and (b) shows the residuals which indicate line emission at 0.65 keV.

column of $N_{\rm H} = 3.96 \times 10^{20}$ cm^{-2}) and a Raymond-Smith model with cosmic abundances and a plasma temperature given by $kT = 0.6$ keV (in good agreement with the canonical model described in Serlemitsos et al. (1996) for a sample of LINERs and starburst galaxies). In (b) we show the residuals which are consistent with line emission from OVIII at 0.65 keV and the Fe-L complex at 0.8–1.0 keV (Serlemitsos et al. 1996). Using these models to calibrate the *ROSAT* counts we find a luminosity for the power-law of 1.6×10^{34} W, and for the plasma model 1.2×10^{34} W. The difference between these and the luminosity calculated from the *Einstein* data may be due partly to the uncertainty of the model parameters.

We consider the merits of these two models and their relevance for starbursts. A power-law model is used for analysing Seyfert galaxies, when the photon index is typically $\Gamma = 2.3 \pm 0.7$ (Boller et al. 1992). The emission line ratios and extended nature of the X-ray flux show that this is clearly not the case here. The X-ray emission in starburst galaxies may be powered by massive X-ray binaries, for which we would expect $0.8 \leq \Gamma \leq 1.5$ (Nagase 1989). Nagase also points out that the associated absorbing column densities are typically very high (on the order of 10^{23} cm^{-3}). Our model predicts an absorbing column higher than galactic, but it is harder to reconcile the large photon index with that expected for X-ray binaries. We can estimate the star-formation rate required for this model by following the method of Ward (1988) and assuming the average luminosity of an X-ray binary to be 10^{31} W. If we take the lifetime of such a binary to be 4×10^4 yr (Fabbiano et al. 1982) we find that a new binary is needed every 25 years.

Alternatively, if the X-rays arise from supernovae, the Raymond-Smith model for hot plasma would be more appropriate. We approach the problem by adopting an average X-ray luminosity of 10^{30} W per supernova remnant, and a typical lifetime of $5\text{–}10\times10^3$ yr (Fabbiano et al. 1982, Rephaeli et al. 1995). The supernova rate is then 1.2–2.4 yr^{-1}.

Any realistic solution is likely to be a combination of both of these processes. In order to estimate the relative contributions, we can find the supernova rate that would be associated with the creation of a massive X-ray binary every 25 years. If one X-ray binary occurs for every 500 OB stars (Fabbiano et al. 1982), then even if only 1/4 of these stars are supernova progenitors (assuming a Salpeter IMF in the range 3–100 $M_\odot$ for OB stars) we find that the X-ray emission from supernovae must dominate over that from X-ray binaries. Although there will inevitably be a considerable scatter in the quantities we have used in our estimates as they depend strongly on the environment, we conclude that the parameters of the Raymond-Smith model, which is applicable to supernova remnants, provide a more consistent solution to the interpretation of the X-ray emission.

5 DISCUSSION

5.1 Spectral Energy Distribution

The spectral energy distribution is shown in Figure 8. Our calibration of the *Einstein* X-ray counts are represented by a bow-tie showing the uncertainty in the X-ray hardness. The optical and UV spectra described in this work are included as solid lines. The photometry in literature is as follows. The radio fluxes are from the Texas survey (365 MHz), Gregory & Condon (1991) (4.85 GHz), and Condon et al. (1990) (1.49 GHz). The spectral index between the 4.85 GHz and 365 MHz fluxes ($F_\nu \propto \nu^{-0.6}$), which both include emission from NGC 7770, is drawn as a dotted line. The 1.49 GHz flux of 124 mJy is integrated over NGC 7771 alone; including NGC 7770 would increase it by 16.5 mJy, not a significant amount as the line joining the first two fluxes also demonstrates. The sub-millimetre data is from Carico et al. (1992) (30 arcsec beam) and Hughes et al. (1997) (typically 16.5 arcsec beam), and far-infrared from the Catalogue of Galaxies and Quasars in the IRAS Survey (Lonsdale et al. 1988). The near-infrared data is from Carico et al. (1991) (5 arcsec aperture) and Eales et al. (1990) (1.4 arcsec and 4.7 arcsec) The UBV photometry is from the 3$^{\rm rd}$ Reference Catalogue of Bright Galaxies (de Vaucouleurs et al. 1991).

It is immediately clear from Figure 8 that the far-infrared dominates the energy output with an enormous implied formation rate of massive stars. Some authors (e.g.

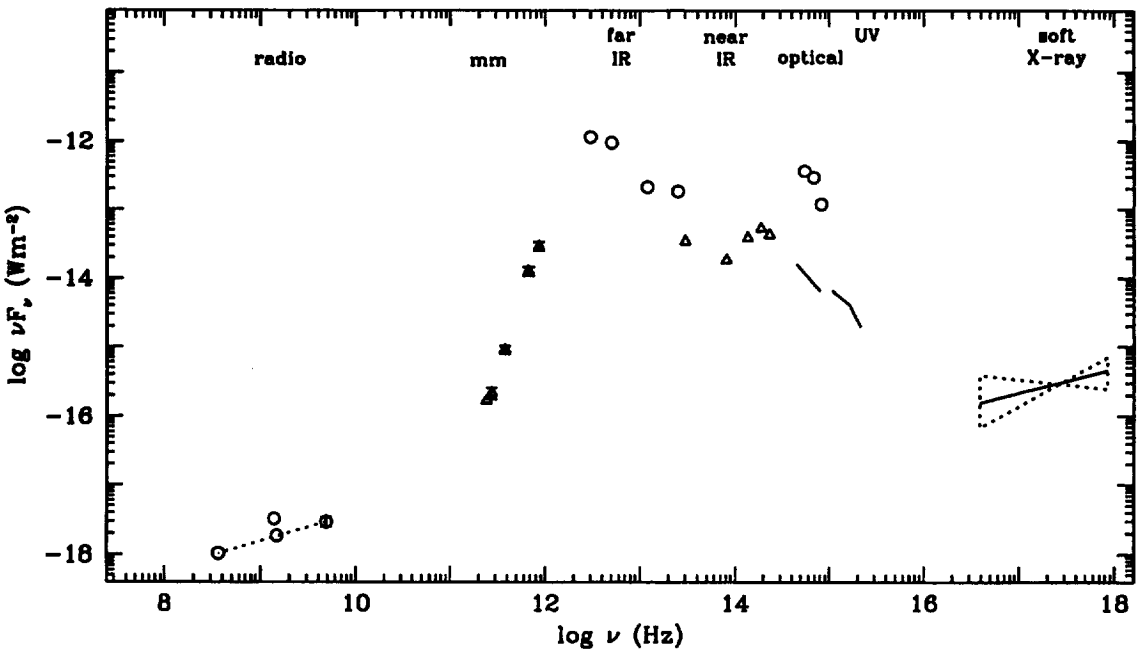

Figure 8. Spectral energy distribution of the galaxy. Circles denote fluxes measured through a large aperture, typically the whole galaxy; triangles denote smaller aperture ($\lesssim$20 arcsec) fluxes; the two solid lines show the new optical and UV spectra; the bow-tie represents the *Einstein* X-ray flux and the uncertainty of its hardness; the dotted line indicates a radio power-law.

Sauvage & Thuan 1992) have argued that a significant fraction of this luminosity is cirrus, and not related to such star formation at all. They claim that the decrease in $L_{\rm FIR}/L_{\rm H\alpha}$ with Hubble type for spiral galaxies depends on the relative contribution from the cirrus component. Hughes et al. (1997) have shown that in NGC 7771 the coolest component of the dust re-radiation accounts for 3/4 of the total (8–1000 μm) infrared emission. If this is dominated by cirrus, the nuclear starburst itself may be responsible for only 1/4 of the infrared luminosity. However, due to the uncertainty and debate about this issue we have not tried to determine the cirrus contribution. As the cirrus must be heated by starlight we can, by using the whole infrared luminosity from 8–1000μm, measure the total star-formation rate including both the starburst and the continuous background rate for the galaxy. This will provide an estimate which may be more reliably compared to those derived from the total radio and total X-ray fluxes.

A further complication arises because the resolution of the X-ray and far-infrared observations is insufficient to clearly distinguish NGC 7770 from NGC 7771. For the discussion in the rest of this Section we have included both of these unless explicitly stated.

An important quantity for starbursts is the supernova rate ($\nu_{\rm SN}$), reflecting the scale of the massive star formation, which we are able to estimate in several ways. We have already seen that the X-ray flux implies $\nu_{\rm SN} = 1$–2, and we now look at that derived from the radio continuum. The radio spectral index between the 4.85 GHz and 365 MHz fluxes is $\alpha = 0.6$ ($F_\nu \propto \nu^{-\alpha}$), consistent with the radio emission being entirely non-thermal synchrotron radiation from shocks in supernovae. There will be a small component of thermal (free-free) emission in the ionised nebulae, but without a measurement of the total Hα flux we can only constrain $\nu_{\rm SN}$ with an upper limit. Condon and Yin (1990) discuss the supernova rate implied by the non-thermal radio flux and argue that

$$\nu_{\rm SN}({\rm yr}^{-1}) \approx \frac{L_{\rm NT}({\rm W\ Hz}^{-1})}{1.3 \times 10^{23}\ \nu^{-\alpha}({\rm GHz})}$$

which yields $\nu_{\rm SN} = 1.2\ {\rm yr}^{-1}$, or for NGC 7771 alone $1.0\ {\rm yr}^{-1}$.

An alternative is to look at the total infrared flux (8-1000μm), which can be found to within $\sim$5% (ignoring uncertainties in the measurements) from the IRAS data using the prescription of Perault (1989). For NGC 7771 and NGC 7770 combined it is $4.3 \times 10^{11} L_\odot$. To calculate the the star-formation rate (SFR) and supernova rate from this we will use the evolutionary synthesis models of Leitherer & Heckman (1995). Complications arise due to the metallicity which can have significant affects, but in the absence of any evidence to the contrary we shall assume solar abundances throughout. The star-formation history is one of the most important parameters, particularly whether it is continuous and if so how long it has been progressing. Although the starburst covers a region 3 kpc across, recent *HST* images (eg Meurer et al. 1995) have shown that in many cases the star-formation occurs in smaller clusters. The overall effect is for continuous star-formation over a larger region. The high supernova rates derived from the X-ray and radio fluxes imply that the star-formation has been progressing long enough for even 8–10 $M_\odot$ stars (which account for most of the supernovae) to evolve away from the Main Sequence. We therefore assume star-formation has been progressing for around 10^8 yrs. The models show that by this time, a sort of steady-state has been reached, and the parameters change very little with time. We find that for a Salpeter IMF in the

range 1–100 $M_\odot$, $SFR = 25\ M_\odot\ yr^{-1}$ and $\nu_{SN} = 0.5\ yr^{-1}$ rather less than those derived from the radio continuum and X-ray flux.

We can use ν_{SN} to estimate the total Hα flux in NGC 7771 as $2\text{–}3 \times 10^{-14}$ W m^{-2}. From our measurement of the extinction corrected Hα surface brightness in Section 2.2 we find this would mean the starburst extends over an area on the order of 60 kpc^2 or around 20 × 20 arcsec, significantly more than is implied by the 7.5 arcsec extent of the line emission along the slit. Carico et al. (1988) have shown that the ratio for 10μm flux within a 4.6 arcsec aperture to the IRAS 12 μm flux (colour corrected to 10 μm) is only 0.17. Since the 10μm emission is believed to be re-radiation from hot dust, it will trace the distribution of the OB stars heating it, and hence implies that the stars responsible are spread out. The radio morphology is also clearly extended along the major axis, although at a much weaker level than the nuclear emission. However, neither of these of these observations can be reconciled with the implied extent of Hα emission, and so we consider the starburst in more detail.

5.2 Equivalent Width of Hα

The equivalent width (EW) of Hα emission is a useful diagnostic of the starforming region. In particular it is independent of the extinction, and is less affected by stellar absorption lines than is the Hβ emission. Our observed value of $EW_{H\alpha} \sim 100$ Å is somewhat lower than expected: a standard IMF with continuous star-formation will produce $EW_{H\alpha} > 100$Å. We therefore discuss some possible causes for this discrepancy, beginning with the geometry. Recent *HST* images of starburst galaxies have shown that star-formation often occurs in many individual compact clusters. The effect of observing at low spatial resolution is for the presence of an underlying stellar continuum to reduce the equivalent widths of emission lines. However, in this case it cannot be significant as the underlying continuum contributes only 10–20 per cent of the total continuum in the region where we detect emission line flux (see Figure 2). The near-infrared spectrum of Smith et al. (1996) shows a low equivalent width for the Brγ line, but this is expected since the contribution from an old population of stars is much more important at 2 μm. The spectrum is indeed characterised by strong CO absorption longward of 2.3 μm, indicating that the effect described above is quite significant at that wavelength.

Another important consideration is whether the nebulae are ionisation bounded or density bounded. The former assumption simplifies the analysis of emission lines, but there is some evidence that a significant number of the UV photons could escape the star-forming cloud without being absorbed, as has been suggested for NGC 4214 by Leitherer et al. (1996). In such cases the size of the HII region is limited not by the number of ionising photons but by the amount of gas available which can be ionised, so although there may be O stars producing a large Lyman continuum (Lyc) flux, the observed Balmer line fluxes are all less by a constant factor (leaving line ratios unaltered). On the other hand, since the ionisation potential for O^+ of 35.1 eV is higher than the 13.6 eV for H^0, the [OIII] lines originate from much closer to the star cluster, and so are unlikely to be truncated in the same way as the hydrogen lines. Thus for the same Lyc flux, a density bounded nebula would have a higher ratio of [OIII]/Hα than an ionisation bounded nebula. Observation of a low ratio strengthens the evidence for a lack of O stars. The UV continuum leads us to a similar conclusion since, as discussed in Section 3, the observed continuum has the same shape as the intrinsic continuum which indicates an origin from A or B type stars.

The third possibility we consider is that dust mixed within the nebulae is competing for UV photons, another effect which is not detectable from Balmer line ratios. Although this may be more significant than extinction beyond the limits of the nebula, it is often ignored and may be why models sometimes over-estimate the Balmer line fluxes, particularly in young starbursts. Wood & Churchwell (1989) compared the radio contiuuum and far-infared fluxes in a number of ultra-compact HII regions, and concluded that 50–90 per cent of the Lyman continuum photons were absorbed by dust internal to the nebulae. It may be that the discrepancy between the estimated total Hα flux and the measured surface brightness can be resolved if 80–90 per cent of the Lyc photons are absorbed by dust internal to HII regions in NGC 7771. Dust absorption of Lyc photons is important even at optical extinctions low enough that relatively few [OIII] and Hα photons are absorbed. Since the [OIII] line originates in only the inner most part of the HII region where the temperature is probably high enough to evaporate dust grains, its flux will be only marginally affected by internal dust. On the other hand the Hα line is produced throughout the nebula and *will* be attenuated, by absorption of Lyc photons. Thus for the same emitted Lyc flux, a dusty nebula will have a higher [OIII]/Hα than a nebula with no internal dust. Again, observation of a low ratio strengthens the evidence for a lack of O stars.

Next we construct a synthetic spectrum using a stellar library to match the starburst in Region 1, after correction for the evolved stellar population in the galaxy's bulge. To do this we extracted a third spectrum from the region 5.25–9.75 arcsec northeast of the centre which we showed to have an old red population (see Section 2.2). After correcting for the different aperture sizes, this spectrum was subtracted from that of Region 1 assuming that they both suffer the same extinction of $A_V = 1.9$ mag. The result was compared to the synthetic spectrum after it had also been reddened by $A_V = 1.9$ mag, as shown in Figure 9. We find that the population of the starburst is consistent with domination by B stars. Any attempt to include O stars in the simulation would then also require the inclusion of K or M stars to retain the slope of the continuum, but the spectrum shows little evidence for absorption features associated with such stars. The scenario of a population dominated by B type rather than O type stars, is consistent with the low [OIII] flux and [OIII]/Hα ratio, as well as the slope of the UV continuum.

A simple explanation for the dearth of O-stars is that starburst is older than a typical O-star, and that starformation has now ceased. Models such as the one described can be used to estimate the time evolution of $EW_{H\alpha}$, including contributions to the continuum from the nebular emission as well as the starburst population. Alonso-Herrero et al. (1996) include a contribution from an evolved underlying stellar population, but as we have discussed this is not significant at optical wavelengths for NGC 7771. We find that

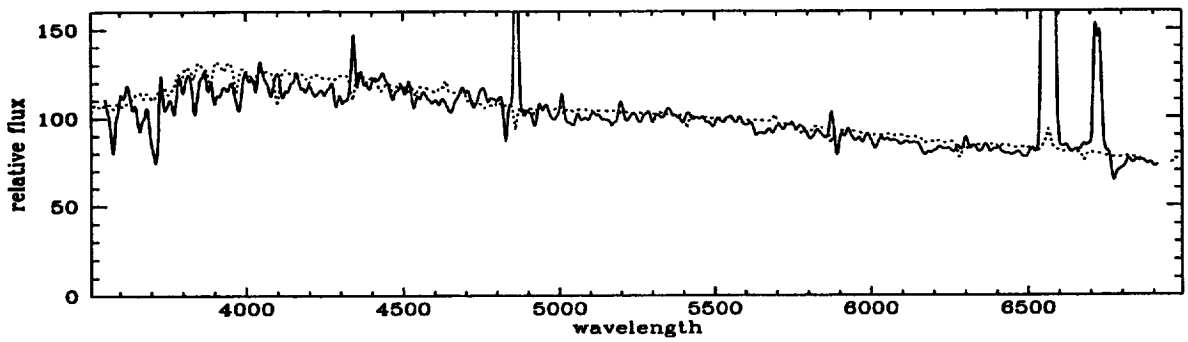

Figure 9. Solid line: spectrum of the starburst (Region 1) with the evolved bulge population subtracted. The short wavelength end (< 4000 Å) in particular is dominated by the noise from the latter. Dotted line: synthetic spectrum of 3 types of B star from the library of Silva & Cornell (1992) with $A_V = 1.9$ magnitudes of extinction. Contributions to the flux at 5450 Å are 60 per cent B5III, 20 per cent B1I, and 20 per cent B8I.

in order to predict $EW_{H\alpha} \sim 100$ Å the starburst must have ceased 6–8 million years previously.

One problem with this idea is that the optical morphology suggests that it is a merger in its early stages (Section 5.4), typical of systems in which star-formation is just beginning rather than ending. The barred gravitational potential acts so as to drive gas inwards by removing angular momentum. The resulting increase in the cloud collision rate, which is proportional to the square of the cloud number density, has two effects: giant molecular clouds are more likely to be formed by coalescence, and compression induced cloud collapse is enhanced (see for example Telesco et al. 1991, and a review of the emipirical law $SFR \propto \rho_{gas}^n$ with $1 < n < 2$ in Kennicutt 1989). The result of this widespread density increase is that star-formation occurs over very extended scales.

What process might stop this star-formation? Clearly, if the gas supply ceases, so will the star-formation, but NGC 7771 has gas in abundance. The mass of molecular hydrogen is estimated from the CO luminosity (measured with a 55 arcsec beam) to be $\log(M_{H_2}/M_\odot) = 10.3$ (Sanders et al. 1991). An alternative might be a superwind created by the piling up of efficiently thermalised supernovae which could ionise the ISM, and perhaps the ensuing mass outflow could halt the inflow. Superwinds are discussed in detail by Heckman et al. (1990) who find outflows along a galaxy's minor axis, and therefore this is unlikely to hinder the inflow of fresh gas in the disk plane. We nevertheless examine the evidence for a superwind in NGC 7771. Note: unfortunately the orientation of the slit is not ideal for observing a wind along the galaxy's minor axis. One piece of evidence would be optical emission lines with ratios indicating shock-heated gas, in particular strong [SII] and [OI] lines. Table 2 gives $[SII](\lambda6716 + \lambda6731)/H\alpha = 0.18$ and $[OI]\lambda6300/H\alpha = 0.02$, rather less than typical shock-excited values of 0.03–0.50 and 0.25–1.20 respectively. Due to the inclination of NGC 7771 we might also expect to see a kinematic signature of double peaked line profiles with a line splitting of 200-600 km s^{-1}, this is not observed. From the correlations in Heckman et al. (1990) between line strength and width we would predict line widths around 50 km s^{-1}, consistent with some of our observations, but implying very little mass outflow. Finally we recall that the Hα flux is associated with a strong blue continuum, which would not be the case if the line emission has an origin in shock heated gas rather than stars. Thus, at least in the central few kiloparsecs, a superwind is not dynamically or radiatively important. We also consider X-ray emission, which would be produced in a wind-blown cavity that has been heated to around 10^7 K. Although the resolution of the X-ray image is limited, it shows evidence for extended emission *along* the disk (as does the radio continuum), indicating star-formation within the bar, rather than perpendicular to the disk on the scale of tens of kiloparsecs as seen in some outflows. Thus we can say that a wind, if present at all, does not dominate the kinematics and luminosity of NGC 7771.

We therefore consider that unusual conditions would be required to halt the star-formation in its early stages, and conclude that it is still in progress. The corollary of this is that the starburst cannot be forming very massive stars.

5.3 Truncated Mass Function

From the evidence we have discussed in the previous section, we conclude that there are far fewer O stars than would normally be found in a starburst. This conclusion is based on several lines of argument: (1) the low equivalent width of Hα which cannot be explained in terms of geometry, density bounded nebulae, or dust absorption within the nebulae; (2) the weak [OIII] lines, implying that the UV radiation field is not hot enough to ionise much O^+; (3) the UV continuum being very weak and having a slope typical of A or B stars; (4) the optical continuum of the star-forming region being dominated by B stars. Further we find no evidence that the star-formation should have ceased, and are led to conclude that no O stars are being made.

We have re-calculated the starburst parameters for a Salpeter IMF but using an upper mass cutoff of $30M_\odot$ for the model described previously and find that with continuous star-formation we can reproduce $EW_{H\alpha} \approx 100$ Å.

If we again assume constant star-formation on timescales of 10^8 yrs then $\nu_{SN} \sim 0.8$ yr^{-1}, in much bet-

ter agreement with the radio and X-ray estimates than before. The lower mass limit of $1M_\odot$ used in the models gives $SFR \sim 40\ M_\odot\ \mathrm{yr}^{-1}$; the effect of having a lower mass limit of 0.1 $M_\odot$ would be to increase the mass of stars formed without significantly affecting the luminosity. We can investigate the importance of this by considering the total mass of stars formed, assuming that stars greater than 8 $M_\odot$ return all their mass to the interstellar medium (ISM) via winds and supernovae, while stars less massive than this effectively have all their mass removed from the ISM permanently. A lower mass limit of $M_l = 1\ M_\odot$ would mean that 75 per cent of the burst mass is retained in stars, leading to a depletion by about 15 per cent of the current gas mass. Similarly we find that for $M_l = 0.1\ M_\odot$, as much as 90 per cent of the burst mass is removed permanently as it is tied up in low mass stars, but still leading to a depletion of only 20 per cent of the gas mass over the same period. The large reserves of molecular hydrogen available suggest that either of these scenarios is equally feasible.

The total Hα flux should be less than before since the most massive stars that dominated the ionising flux are no longer included in the calculation. We estimate it as 4.3×10^{-15} W m^{-2}, which would extend over an area of 60 arcsec^2 for our measurement of the Hα surface brightness. If we assume that the emission is extended by similar amounts both along and perpendicular to the slit, then this measurement is completely consistent with the observed extent of 7.5 arcsec.

5.4 Interaction

NGC 7771 is part of an interacting system, being closely associated with NGC 7770 which is a smaller face-on galaxy. Their nuclei are separated by only 65 arcsec, a projected distance of 27 kpc, and their redshifts differ by $\sim$350 km s^{-1}. Veilleux et al. (1995) have presented long-slit data on this galaxy (denoted by them NGC 7771 S) which show it has a similar Hα surface brightness, 27×10^{-17} W m^{-2} in a 2 arcsec$\times$2 arcsec aperture and corrected for $A_V = 1.8$ mag extinction. The extent of this starburst is unknown, but the radio continuum shows the total flux is only about 10 per cent of that in NGC 7771.

Mihos & Hernquist (1994) have modelled 'minor merger systems' which involve a disk galaxy accreting a low-mass companion. The tidal perturbations induced by the satellite can cause the disk galaxy to develop a two-armed spiral pattern which drives a substantial fraction of the disk gas towards the central regions, triggering star formation. The presence of a bulge in the disk galaxy will help to stabilise the disk against strong inflow so that the final nuclear starburst is less compact.

Qualitatively, this model describes the situation in NGC 7771 reasonably well. It is interacting with a smaller galaxy, and it does appear to have a two-armed spiral; there is star-formation occuring weakly throughout the galaxy and in a much greater concentration towards the centre; the starburst is certainly not compact, covering as it does a region more than 3 kpc across.

We now attempt to explain the existence of the cluster of non-ionising stars that are obscuring part of the nuclear starburst. This could be due to resonances associated with a barred gravitational potential. If we consider the epicyclic approximation for stellar orbits, where a retrograde elliptical motion is superimposed on a prograde circular orbit, the stars at some radius r will have an angular velocity $\Omega(r)$ perturbed by an epicyclic frequency $\kappa(r)$ where $\kappa(r)^2 = r\frac{\mathrm{d}\Omega^2}{\mathrm{d}r} + 4\Omega^2$ (see Binney & Tremaine 1987, Combes et al. 1995); we denote the pattern speed of the slowly rotating bar to be Ω_b. If inner Lindblad resonances were to exist they would do so where $\Omega_b = \Omega(r) - \kappa(r)/2$, although as this appears not to be so then at all radii $\Omega_b > \Omega(r) - \kappa(r)/2$. The stars will also be oscillating perpendicular to the plane according to $\ddot{z} = -\nu_z^2 z$ where the frequency ν_z is related the gravitational potential $U(r,z)$ by $\nu_z^2 = \frac{\partial U(r,0)}{\partial z^2}$ (Combes et al. 1995). There will be resonances, analogous to the Lindblad resonances, when stars cross the disk plane in approximately the same position relative to the bar each time, ie $\Omega_b = \Omega(r) - \nu_z(r)/2$. This can be at a different radius to the Lindblad resonances, and can be satisified even if the criterion for Lindblad resonances is not. It has been used to explain the peanut-shape of some edge-on galaxies, and in principle it could be that the obscuring cluster is a deformation due to such a resonance. The scenario would account for the higher velocity dispersion for the emission lines in this region. The typical timescale for the stars to travel a distance on the order of 1 kpc above the disk plane (similar to their distance from the centre in the plane), with a typical velocity of 100 km s^{-1} (from Section 2.3) is 10^7 years, sufficient for stars more massive than ~ 10 M$_\odot$ to have evolved away from the Main Sequence. Thus we would expect, as is observed, that the obscuring stars do not include any with strong ionising fluxes.

6 CONCLUSION

We present new optical and UV spectra, and a soft X-ray image and spectrum, which are analysed in conjunction with data taken from the literature, covering the entire spectral energy distribution of the galaxy.

The optical spectrum has shown that there is a large starburst in the nucleus of NGC 7771 that is partially hidden by a cluster of non-ionising stars. Although the infrared (8–1000 μm) and soft X-ray emission are confused by the proximity of NGC 7770, the radio flux shows that this latter galaxy makes only a small contribution. Thus we can adopt a supernova rate of 0.8–1 yr^{-1} as indicated by these three fluxes. The estimated total Hα flux is consistent with the measured Hα surface brightness and its extent along the slit, assuming that the emission is extended a similar amount perpendicular to the slit.

The low equivalent width of Hα, on the order of 100 Å, is apparently at odds with the high current star-formation rate. By also considering other evidence — namely the weak [OIII] lines, the shape and weakness of the UV continuum, and the shape of the optical continuum in the starburst — we have argued that this cannot be due to effects of geometry, density bounded nebulae or dust absorption within the nebulae. Modelling the starburst with a standard IMF indicates that the star formation episode must have concluded several million years previously, a result that is inconsistent with the large mass of available gas and the dynamical state of the galaxy. We conclude that the initial mass function is truncated, with $M_u = 30M_\odot$.

NGC 7771 is in the early stages of a merger, the massive burst of star formation currently in progress apparently having been caused by tidal interaction with the nearby dwarf galaxy NGC 7770. This interaction has given rise to a barred potential which is driving gas inwards and fuelling the starburst. The bulge in NGC 7771 acts as a regulator, opposing the inflow caused by the interaction and hence the star-formation is extended over several kiloparsecs. This may also cause the anomalously low fraction of massive stars compared to the standard picture of a starburst.

Near the centre there is a resonance, analogous to Lindblad resonances but perpendicular to the disk plane. This is causing stars in the region to oscillate out of the plane more vigorously and gives rise to what appears to be a cluster of stars obscuring part of the starburst. The timescale for the stars to move out of the plane acounts for the lack of ionising stars in this cluster.

7 ACKNOWLEDGEMENTS

We thank the anonymous referee for helpful comments on how to improve this paper. RID acknowledges the support of a PPARC (EPSRC) research studentship grant; AA-H was partially supported by the National Aeronautics and Space Administration on grant NAG 5-3042 through the University of Arizona. This research has made use of the NASA/IPAC Extragalactic Database (NED) which is operated by the Jet Propulsion Laboratory, California Institute of Technology, under contract with the National Aeronautics and Space Administration; and also of data obtained through the High Energy Astrophysics Science Archive Research Center Online Service, provided by the NASA-Goddard Space Flight Center.

REFERENCES

Achtermann J.M., Lacy J.H., 1995, ApJ, 439, 163
Alonso-Herrero A., Aragón-Salamanca A., Zamorano J., Rego M., 1996, MNRAS, 278, 417
Binney J., Tremaine S., 1987, in Galactic Dynamics (Princeton University Press)
Boller Th., Meurs E. J. A., Brinkmann W., Fink H., Zimmerman U., Adorf H.-M., 1992, A&A, 261, 57
Carico D. P., Sanders D. B., Soifer B. T., Elias J. H., Matthews K., Neugebauer G., 1988, AJ, 95, 356
Carico D. P., Keene J., Soifer B.T., Neugebauer G., 1992, PASP, 104, 1086
Charlot S., Ferrari F., Matthews G., Silk J., 1993, ApJ, 419 L57
Combes F., Boissé P., Mazure A., Blanchard A., 1995, in Galaxies and Cosmology (Springer-Verlag)
Condon J. J., Helou G., Sanders D. B., Soifer B. T., 1990, ApJS, 73, 359
Condon J. J., Yin Q. F., 1990, ApJ, 357, 97
Doyon R., Puxley P. J., Joseph R. D., 1992, ApJ, 397, 117
Eales S. A., Becklin E. E., Hodapp K.-W., Simons D. A., Wynn-Williams C. G., 1990, ApJ, 365, 478
Evans I. N., Dopita M. A., 1985, ApJS, 58, 125
Fabbiano G., 1989, ARAA, 27, 87
Fabbiano G., Feigelson E., Zamorani G., 1982, ApJ, 256, 397
Fabbiano G., Kim D.-W., Trinchieri G., 1992, ApJS, 80, 531
French H. B., 1980, ApJ, 240, 41
Fruscione A., Griffiths R.E., 1991, ApJ, 380, L13
Gehrz R. D., Sramek R. A., Weedman D.N., 1983, ApJ, 267, 551
Gregory P. C., Condon J. J., 1991, ApJS, 75, 1011
Heckman T. M., Armus L., Miley G. K., 1990, ApJS, 74 833
Hughes D. H., Ward M. J., Davies R. I., 1997, MNRAS, in preparation
Kim D.-C., Sanders D. B., Veilleux S., Mazzarella J. M., Soifer B. T., 1995, ApJS, 98, 129
Kinney A. L., Bohlin R.C., Calzetti D., Panagia N., Wyse R. F. G., 1993, ApJS, 86, 5
Leitherer C., Heckman T.M., 1995, ApJS, 96, 9
Leitherer C., Vacca W., Conti P., Filippenko A., Robert C., Sargent W., 1996, ApJ, 465, 717
Lonsdale C. J., Helou G., Good J. C., Rice W., 1988, Catalogue of Galaxies and Quasars in the IRAS Survey
Meurer G.R., Heckman T.M., Leitherer C., Kinney A., Robert C., Garnett D.R., 1995, AJ, 110, 2665
Mihos J., Hernquist C., 1994, ApJ, 425, 13L
Nagase F., 1989, PASJ, 41, 1
Perault M., 1989, PhD thesis, Univ Paris
Puxley P.J., Brand P.W.J.L., Moore T.J.T., Mountain C. M., Nakai N., Yamashita T., 1989. ApJ, 345, 163
Rephaeli Y., Gruber D., Persic M., 1995, A&A, 300, 91
Rieke G.H., Lebofsky M.J., Thompson R.I., Low F.J., Tokunaga A.T., 1980, ApJ, 238, 24
Rieke G.H., Loken K., Rieke M., Tamblyn P., 1993, ApJ, 412, 99
Sanders D.B., Scoville N.Z., Soifer B.T., 1991, ApJ, 370, 158
Sauvage M., Thuan T.X., 1992, ApJ, 396, L69
Scalo J. M., 1989, in Renzini A., Fabianno G., Gallagher J. S., eds, Windows on Galaxies. Kluwer, Dordrecht, p.125
Serlemitsos P., Ptak A., Yaqoob T., 1996, preprint
Shields J. C., 1993, ApJ, 419, 181
Silva D. R., Cornell M. E., 1992, ApJS, 81, 865
Smith D.A., Herter T., Haynes M.P., 1996, ApJS, 104, 217
Soifer B.T., et al., 1987, ApJ, 320, 238
Storchi-Bergmann T., Kinney A., Challis P., 1995, ApJS, 98, 103
Telesco C.M., Dressel L., Wolstencroft R., 1993, ApJ, 414, 120
de Vaucouleurs G., de Vaucouleurs A., Corwin H. G., Buta R. J., Paturel G., Fouqué P., 1991, 3rd Reference Catalogue of Bright Galaxies
Veilleux S., Kim D.-C., Sanders D. B., Mazzarella J. M., Soifer B.T., 1995, ApJS, 98, 171
Ward M. J., 1988, MNRAS, 231, 1P
Weedman D. W., Feldman F. R., Balzano V. A., Ramsey L. W., Sramek R. A., Wu C.-C., 1981, ApJ, 248, 105
Wood D.O.S., Churchwell E., 1989, ApJS, 69, 831
Wright G. S., Joseph R. D., Robertson N. A., James P. A., Meikle W. P. S., 1988, MNRAS, 233, 1